Title
DEFORMATION BEHAVIOUR AND SHAPE MEMORY EFFECT OF NEAR EQUIATOMIC NiTi ALLOY

Author
Mohamed, H.A.

Publication Date
1977-03-01

Submitted to Journal of Materials Science

LBL-5141
Preprint C

DEFORMATION BEHAVIOUR AND SHAPE MEMORY EFFECT OF NEAR EQUIATOMIC NiTi ALLOY

H. A. Mohamed and J. Washburn

March 1977

Prepared for the U. S. Energy Research and Development Administration under Contract W-7405-ENG-48

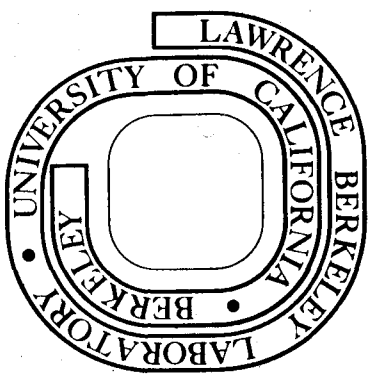

DISCLAIMER

DEFORMATION BEHAVIOUR AND SHAPE MEMORY EFFECT OF NEAR EQUIATOMIC NiTi ALLOY

H. A. Mohamed and J. Washburn
Materials and Molecular Research Division, Lawrence Berkeley Laboratory and
Department of Materials Science and Engineering, College of Engineering
University of California, Berkeley, California 94720

ABSTRACT

The mechanical shape memory effect associated with the martensitic-type transformation which occurs in polycrystalline Ti-50.3 at. pct. Ni alloy has been investigated using the techniques of transmission and optical microscopy. Deformation of initially partially transformed material within the recoverable strain range was found to occur by: (i) stress-induced transformation of the most favorably oriented existing martensite variants at the expense of adjacent unfavorably oriented variants and retained high temperature phase (ii) stress-induced re-orientation of favorably oriented martensite by utilizing the most favorably oriented twin system and (iii) stress-induced twin boundary migration within the martensite. The reverse transformation during heating restores the original grain structure of the high temperature phase in a highly coherent manner. It was concluded that deformation modes limited to those involved in the transformation process and the reversibility of the transformation give rise to the memory effect.

INTRODUCTION

The mechanical shape memory effect is a phenomenon exhibited by several alloys which undergo thermoelastic martensitic-transformation. For detailed discussions of shape memory alloys, the reader may consult reference [1]. Of particular interest is the alloy Ni-Ti near the equiatomic composition. The classical demonstration of the memory effect is to bend an object made out of the material at a temperature below the M_s (martensite start temperature during cooling) and then heat it. During heating the object tends to recover its original undeformed shape. Complete recovery of shape can be attained only after heating to above the A_f temperature (temperature at which reverse transformation to the high temperature phase is completed) and provided that the initial strain did not exceed a certain critical value, otherwise, recovery of shape would be incomplete.

The deformation behaviour of near equiatomic Ni-Ti alloys and its relation to the reversible martensitic-transformation which occurs in the vicinity of room temperature have been studied by several investigators [2-13]. Most of this work was concerned with measuring such properties as elastic modulii[2], yield strength [3,5], hardness [10] and their variation within the transformation temperature range, obtaining stress-strain data [3,5,11,12] and studying the effect of transformation cycling on the fatigue strength [8]. Little attempt has been made by Sastri and Makcinkowski[4] to clearly establish the deformation mode(s) in the early stages and correlate these with the microstructural features. However, their result was inconclusive. In order to explain the mechanism of the memory effect it is essential to establish the deformation mode(s) within the recoverable strain range. This is the subject of the present paper.

2. EXPERIMENTAL PROCEDURE

All the specimens (sheets 1mm thick) were solution treated at 1000°C for 24 hrs. in quartz capsules under argon atmosphere, about 10^{-6} torr, and then quenched in ice water. Chemical analysis was done after such treatment since the initial nominal composition might be of little significance in determining properties of experimental specimens [13,14]. This analysis showed that:

Ni	55.4wt. pct. (50.3at. pct.)
O	about 350 ppm
N	less than 10 ppm

The initial M_s temperature (without thermal cycling) as determined from the peak of the electrical resistivity vs. temperature diagram [16] was found to be about 55°C. At room temperature the material was partially transformed into martensite. Thin foils for transmission microscopy were prepared by a jet polishing technique in a solution containing 1 HNO_3:3 Methanol by volume. The foils were examined in a Siemens IA EM and Philips 100 EM equipped with deformation and hot stages. For in situ deformation experiments, the foils were glued to the holder using Eastman #910 adhesive. All the experiments were carried out at an operating voltage of 100 kV. For optical microscopy, specimens were polished and etched in a solution containing 1 HF : 4 HNO_3 : $5H_2O$ by volume [17] or highly polished only in order to observe surface relief effects during progressive straining.

3. EXPERIMENTAL RESULTS AND DISCUSSION

3.1 Microstructural Features

Figure 1a is an optical micrograph of an etched specimen taken at room temperature. Fine parallel bands within the grains of the high

temperature phase (CsCl-structure) can be seen. These bands are martensite plates as was verified from electron micrographs. Figure 1b is a bright-field image taken at room temperature and showing a zig-zag arrangement of martensite plates. This morphology is typical of self-accommodating martensite. It was very seldom that an isolated martensite plate was observed in the field of view. This suggests that growth of self-accommodating groups of martensite plates is favored over that of individual plates because the former is associated with less macroscopic strain. This type of morphology has been observed in several other alloys e.g., Cu-Al [18], Ag-Cd [19], Cu-Al-Ni [20].

This observation indicates that the strain associated with the transformation and which is to be accommodated by the high temperature phase is minimized. This is consistent with the reversibility of the transformation since if the transformation strain is large enough to cause appreciable slip, the transformation would be irreversible. Selected-area diffraction and dark-field imaging verified that the parallel bands within each member of the group shown in Figure 1b are twin-related along {111} plane of the martensite structure (distorted orthorhombic) as reported for similar NiTi alloys by some other investigators [21,22]. Members of a self-accommodating group of martensite plates are themselves twin-related along {111} plane of the martensite structure as has been verified by trace analysis of electron micrographs and their corresponding diffraction patterns.

Therefore, we can conclude that the martensitic-phase consists of twin-related plates which form self-accommodating groups. These twin-related plates are further subdivided into smaller units which are again twin-related along the same plane. The significance of these observations

is that, as will be shown, the boundaries separating the microstructural units were observed to be mobile under an external stress.

3.2 Deformation Modes in the Early Stages of Initially Partially Transformed Material

Figure 2 shows a true tensile stress-strain diagram obtained at room temperature. This is a typical stress-strain diagram of shape memory alloys [23]. The maximum recoverable strain corresponds to point C. Therefore, in order to explain the mechanism of the memory effect, the deformation mode(s) within stage BC which is characterized by relatively low rate of strain hardening has to be established. Figure 3 is a sequence of optical micrographs showing the surface of a tensile sheet specimen which was initially polished and then deformed in tension at room temperature with a small calibrated tensile device while under optical microscope observation (polarized light). It can be seen that during progressive straining, a group of parallel bands have developed. These are believed to be surface relief effects resulting from stress-induces growth and/or re-orientation of the most favorably oriented existing martensite. It is to be noted that during the course of straining, no new bands have developed. This is probably because the material was partially transformed to martensite (thermally) prior to deformation and since the transformation is thermoelastic [17], growth and/or re-orientation of already existing martensite would be expected to be much more likely than nucleation of new martensite. In view of the observed microstructural features, stress-induced transformation of the most favorably oriented martensite would be expected to occur at the expense of unfavorably oriented martensite and/or retained high temperature phase. Figure 4 shows x-ray diffractometer traces obtained at

room temperature from undeformed and deformed specimens. It can be seen that after giving 3 pct. total elongation at room temperature the "integrated" intensities of (020), $(1\bar{1}1)$ and (002) martensite diffraction lines have increased at the expense of the $(110)_{CsCl}$ "integrated" intensity. This indicates that some growth of already existing martensite has occured at the expense of retained high temperature phase. The deformation behaviour has been further studied on the finer scale of the electron microscope. Figure 5 shows the result of in situ deformation experiment. The foil was imaged in the same area before and after deformation in tension at room temperature under the same diffraction conditions. It can be seen by comparing the two micrographs, that after deformation, the martensite variant marked "A" has grown at the expense of the neighboring variant marked "B".

This observation indicates that the martensite-martensite interface which was found to coincide with the {111} twinning plane is mobile under stress. Further, it can be seen that a new set of thin parallel bands have appeared at C. Probably these fine bands are twins within a martensite variant which has been grown under stress and was outside the field of view prior to deformation. During the course of the in situ deformation experiments it was observed that during deformation, sets of twins within martensite variants have disappeared and been replaced by other sets running in different directions. Sometimes sets intersecting each other were also observed. These observations indicate the complexity of the deformation behaviour on the fine scale. Figure 6 shows that after deformation, only the set of twins at "B" remained parallel to the corresponding set before deformation at "A". Further, this set can be

seen to spread and wipe out the other sets. In addition a new set has appeared and tends to intersect the other set.These observations suggest that several events may occur during deformation.

The lattice-invariant deformation of the transformation is required by the crystallographic theories to minimize the distrotion at the martensite-high temperature phase interface. In the present case this is {111} twinning. The twinning shear direction was determined from the geometry of the martensite structure and the formulae given by Andrews and Johnson [24]. This was found to be close to <123>. It is suggested that, under an external stress, those sets of twins within a martensite variant which are not favorably oriented with respect to the resolved shear of the applied stress would be expected to shrink. The condition that the habit plane should be an invariant plane strain may be satisfied by another {111}<123> twin system. This results in re-orientation of a martensite variant without the need to pass through the high temperature phase as an intermediate step as has been hypothesized by Wasilewski [6,7,9,13].

Figure 7a shows a bright-field image of a twinned martensite plate observed at room temperature. The same area was observed again under the same diffraction conditions after the foil had been slightly bent outside the microscope at room temperature as shown in Figure 7b. The image of b was printed to be the mirror image of a and then both images were cut along the same line. It can be seen by comparing the two images along this common line that one of the two sets of twin-related domains has grown at the expense of the other.

The above results suggest that all the boundaries present in the microstructure are mobile and that deformation in the early stages occurs by:

(a) stress-induced growth of the most favorably oriented existing martensite at the expense of (i) unfavorably oriented adjacent variant by motion of the martensite-martensite interface which coincides with the {111} twin plane and (ii) retained high temperature phase by motion of the martensite-high temperature phase interface toward the retained high temperature phase side.

(b) stress-induced re-orientation of an existing martensite. This involves stress-induced transformation of an existing martensite variant into another of different orientation by utilizing the most favorable twin system.

(c) stress-induced twin boundary migration within a martensite variant. This results in a change in the relative width of the twin-related domains within that variant.

Deformation by preferential growth of ceratin martensite variants at the expense of others has been observed in almost completely transformed Cu-Zn [25,26] and Cu-Zn-Al [27] alloys. Twin boundaries within martensite were also observed to be mobile under stress in In-Tl [28], Au-Cd [29] and Cu-Al-Ni [30] alloys.

3.3 Evidence added in Proof of the above deformation modes

The observed deformation modes in the early stages were further confirmed by an interesting observation. It was found that if a virgin specimen (not cycled) was bent at room temperature and then cooled further, it continued to bend spontaneously in the same direction as

shown schematically in Figure 8. Heating to above about 62°C caused the specimen to completely recover its original undeformed shape. Further cooling in absence of the initial bending did not cause any macroscopic shape change. This behaviour is different from the reversible or two-way shape memory effect [31-36] which seems to require the recoverable strain limit to be exceeded [31-35] or several hundred transformation-deformation cycles [37]. In the latter case, change of shape occurs reversibly during both heating and cooling. The observed spontaneous strain is believed to be related to the observed deformation modes in the following way: since further cooling of a partially transformed specimen causes the martensite plates to grow, those plates which have been preferentially enlarged by the initial bending would thereafter make the major contribution to the new thermally transformed volume. This would contribute to the observed macroscopic strain. Also, further growth of martensite plates in which one set of twins had been widened at the expense of the other set by the initial strain would contribute additional macroscopic strain. These processes are illustrated schematically in Figure 9. It is suggested that the sum of these two strains is the cause of the observed spontaneous strain. Therefore, this strain would be expected to be observed only if the material was only partially transformed prior to the initial deformation. This was taken as a method to determine the M_f temperature. Wire specimens were bent at different temperatures below room temperature and then further cooled. The highest temperature at which bending was applied and then on further cooling the specimen did not spontaneously bend further was taken as the M_f temperature. This was found to be about -90°C.

3.4 Deformation in Latter Stages

Figure 10 shows bright and dark-field images of a foil prepared from a tensile specimen given 8 pct. total elongation at room temperature. The observed microstructure was typical of specimens given relatively large amounts of strain and is representative of deformation within stage DE of Figure 2. It can be seen that the twin boundaries and the martensite plate boundary became highly irregular compared to undeformed specimens and those given small amounts of strain. The microstructure of Figure 10 is to be compared with that of Figure 11 where the foil was prepared from a tensile specimen given 3 pct. total elongation at room temperature. The irregularity of the boundaries of Figure 10 compared to that of Figure 11 suggests that slip has taken place in stage DE. This is also evident from the presence of line features within the martensite in Figure 10. The microstrucutre of specimens deformed within stage CD was very similar to that within stage BC. These results suggest that deformation within stage DE occurs by slip while deformation within CD is an elastic deformation of the martensite configuration formed at C. Specimens given larger than about 6 pct. total elongation at room temperature never recovered their original dimensions upon heating. This is consistent with the observation that deformation within stage DE occurs by slip which is in general irreversible. Slip in the ordered martensite structure would be expected to be a difficult process since it creates anti-phase boundaries and thus it occurs at high stress levels. The difficulty of slip is evident from the fracture mode. Figure 12 shows scanning electron micrographs of the fracture surface. It can be seen that the fracture is mostly intergranular. The fracture

surface was always normal to the tensile axis and no necking was observed.

3.5 Nature of the Reverse Transformation to the High Temperature Phase

Figure 13 shows a sequence of bright-field images and their corresponding selected-area electron diffraction patterns taken during heating from room temperature. It can be seen that during heating the martensite plates shrink in a highly coherent manner until they disappear completely. This is a typical characteristic of thermoelastic martensites and suggests that the martensite-high temperature phase interface is highly glissile as would be expected. This observation indicates that reversion of martensite to the high temperature phase in a thin foil occurs by the same mechanism observed in bulk material [17].

In order to determine whether an almost completely transformed material still exhibits a memory, a wire was bent at liquid nitrogen temperature and then heated. It was found that upon heating to about 70°C., the wire recovered its original undeformed shape. This observation proves that an almost completely transformed material still exhibits a memory and is in agreement with the results of Otsuka et al [17] on 49.75 at. pct. Ni alloy. Figure 14a is an optical micrograph showing the microstructure of an etched specimen at room temperature. Figure 14b shows the same area after the specimen was immersed in liquid nitrogen for 20 minutes, heated to 100°C to revert all the martensite, cooled to room temperature and then slightly re-etched to reveal any microstructural change which might have occured. It can be seen that the specimen had regained its original grain structure, however a slight change in the shape of some grains has occured as can be seen at A. After ten such cycles the effect became more pronounced as can be seen from Figure 14C. By comparing a and c one may notice that there has been migration of

some grain boundaries. Whether this observation reflects a real shift or is due to the effect of re-etching on some boundaries that lie nearly parallel to the surface needs further investigation. The sequence of the micrographs of Figure 14 illustrates that the material even while it is almost completely transformed to martensite, always remembers the original grain structure of the high temperature phase. This suggests that there is a unique path for the atoms to follow during the reverse transformation. Wayman and Shimizu [38] were the first to point out that ordering places a severe restriction on the available lattice correspondences or inverse Bain strain for the reverse transformation. The present case is very similar to the transformation in Au-47.5 at. pct. Cd alloy [39,40] (CsCl-structure → orthorhombic). While there are six equivalent lattice correspondences for the forward transformation to martensite, there is only one correspondence for the reverse transformation. Therefore, the material always remembers the original grain structure of the high temperature phase as is evident from the sequence of micrographs of Figure 14. In addition, the observed microstructural features (self-accommodating groups of martensite plates which are twin-related) suggest that the transformation strain to be accommodated by the high temperature phase is very limited. This transformation mode undoubtedly contributes to the reversibility of the transformation.

3.6 Mechanism of the Memory Effect

It was shown that the deformation modes within the recoverable strain range (stage BC of Figure 2) are limited to those modes involved in the transformation process itself. Further, the reverse transformation occurs by a martensitic mechanism that restores the original grain

structure of the high temperature phase. Therefore, the strain associated with these modes would be expected to be reversed when the martensite reverts to the high temperature phase.

4. CONCLUSIONS

The deformation behaviour and shape memory effect in polycrystalline Ti-50.3 at. pct. Ni alloy have been investigated. From this work the following conclusions could be drawn:

(1) Deformation within the recoverable strain range of a partially transformed material occurs by modes limited to those involved in the transformation process. These are: (i) stress-induced transformation of the most favorably oriented existing martensite variant at the expense of adjacent unfavorably oriented variant and retained high temperature phase. (ii) stress-induced re-orientation of martensite by utilizing the most favorably oriented twin system. (iii) stress-induced twin-boundary migration within a martensite variant.

(2) The reverse transformation during heating occurs in a highly coherent manner that restores the original grain structure of the high temperature phase.

(3) The memory effect arises from: (i) reversibility of the transformation and (ii) the limitation of deformation modes within the recoverable strain range to those involved in the transformation process itself.

ACKNOWLEDGEMENTS

This work was supported by the National Science Foundation and the United States Energy Research and Development Administration. Any conclusions or opinions expressed in this report represent solely those of the authors and not necessarily those of The Regents of the University of California, the Lawrence Berkeley Laboratory or the United States Energy Research and Development Administration.

REFERENCES

1. J. Perkins, ed., Shape Memory Effects in Alloys, Plenum Press, New York, 1975.
2. R. J. Wasilewski, TMS-AIME 233, (1965) 1691.
3. A. G. Rozner and R. J. Wasilewski, J. Inst. Metals, 94 (1966) 169.
4. A. S. Sastri and M. J. Marcinkowski, TMS-AIME, 242 (1968) 2393.
5. W. B. Cross, A. H. Karigits and F. J. Stimler, "Nitinol Characterization Study", NASA Contractor Report (1969) Cr-1433.
6. R. J. Wasilewski, Scr. Met., 5 (1971) 127.
7. R. J. Wasilewski, ibid, 131.
8. R. J. Wasilewski, ibid, 233.
9. R. J. Wasilewski, Met. Trans 2 (1971) 2973.
10. K. Mukherjee, F. Millio and M. Chandrasekaran, Mat. Sci. and Eng., 14 (1974) 143.
11. G. R. Edwards, J. Perkins and J. M. Johnson, Scr. Met., 9 (1975) 1167.
12. J. Perkins. G. R. Edwards, C. R. Such and J. M. Johnson in Shape Memory Effects in Alloys, Plenum Press, New York, 1975, 273.
13. R. J. Wasilewski, in Shape Memory Effects in Alloys, Plenum Press, New York, 1975, 245.
14. C. M. Jackson, H. J. Wagner and R. J. Wasilewski, "55-Nitinol- The Alloy with a Memory, its Physical Metallurgy, Properties and Applications", NASA Report (1972) SP 5110.
15. R. J. Wasilewski, S. R. Butler, J. E. Hanlon and D. Warden, Met. Trans 2 (1971) 229.
16. G. D. Sandrock, A. J. Perkins and R. F. Hehemann, Met. Trans., 2 (1971) 2769.

17. K. Otsuka, T. Sawamura, K. Shimizu and C. M. Wayman, Met. Trans. 2 (1971) 2583.

18. H. Tas, L. Delaey and A. Deruyttere, Met. Trans., 3 (1973) 2833.

19. L. Delaey, R. V. Krishnan, H. Tas and H. Warlimont, J. Mat. Sci., 9 (1974) 1521.

20. K. Otsuka and K. Shimizu, Trans. Jap. Inst. Metals, 15 (1974) 103.

21. K. Otsuka, T. Sawamura and K. Shimizu, phys. stat sol. 5a (1971) 457.

22. S. P. Gupta and A. A. Johnson, Trans. Jap. Inst. Metals, 14 (1973), 292.

23. R. V. Krishnan, L. Delaey, H. Tas and H. Warlimont, J. Mat. Sci., 9 (1974) 1536.

24. K. W. Andrews and W. Johnson, Brit. J. Appl. Phys., 6 (1955) 92.

25. T. A. Schroeder, I. Cornelis and C. M. Wayman, Met. Trans. 7A (1976) 535.

26. T. A. Schroeder and C. M. Wayman, Scr. Met., 10 (1976) 241.

27. K. Takezawa, T. Shindo and S. Sato, ibid, 13.

28. Z. S. Basinski and J. W. Christian, Acta Met., 2 (1954) 101.

29. H. K. Birnbaum and T. A. Read, TMS-AIME, 218 (1960) 662.

30. K. Otsuka, Jap. J. Appl Phys., 10 (1971) 571.

31. H. Tas, L. Delaey and A. Deruyttere, J. Less Common Met., 28 (1972) 141.

32. A. Nagasawa, K. Enami, Y. Ishino, Y. Abe and S. Nenno, Scr. Met. 8 (1974) 1055.

33. J. Perkins, ibid, 1469.

34. T. Saburi and S. Nenno, ibid, 1363.

35. R. Oshima and K. Adachi, Jap. J. Appl. Phys., 14 (1975) 563.

36. R. J. Wasilewski, Scr. Met., 9 (1975) 417.

37. Paul Hernandez and Ridgeway Banks, Lawrence Berkeley Laboratory, University of California at Berkeley, Private Communication, 1975.

38. C. M. Wayman and K. Shimizu, Mat. Sci, J., 6 (1972) 175.

39. D. S. Lieberman, Phase Transformation ASM, Metals Park, Ohio, 1970, 1.

40. D. S. Lieberman, M. A. Schmerling and R. W. Karz in Shape Memory Effects in Alloys, Plenum Press, New York, 1975, 203.

Fig. 1. Microstructure of the martensitic phase (a) Optical micrograph (b) bright-field transmission electron micrograph.

Fig. 2. True tensile stress-strain diagram at room temperature.

Fig. 3. Optical micrographs showing surface relief effects associated with stress-induced growth and/or re-orientation of the most favorably oriented existing martensite. (a) 1% (b) 2% and (c) 3% total elongation at room temperature.

Fig. 4. X-ray diffractometer traces of undeformed and deformed specimens (a) Undeformed (b) specimen given 3% total elongation at room temperature.

Fig. 5. Example of in situ deformation stage experiment in the electron microscope showing stress-induced growth of one martensite variant at the expense of other and stress-induced growth at the expense of retained high temperature phase. (a) Before deformation and (b) after deformation.

Fig. 6. Another example of in situ deformation experiment showing stress-induced re-orientation of martensite by utilizing the most favorable twinning mode. (a) Before deformation and (b) after deformation.

Fig. 7. Effect of external deformation on the widths of twin-related domains within a martensite variant. (a) Undeformed and (b) after slight bending at room temperature outside the microscope.

Fig. 8. Schematic illustration showing the spontaneous bending observed during further cooling of a specimen bent slightly at room temperature. (a) Original shape and shape after bending at room temperature (b) and (c) change in shape which occurs with progressive cooling.

Fig. 9. Schematic interpretation of the effect illustrated in Figure 8. (a) Favorably and unfavorably oriented martensite plates before

(dashed lines) and after (solid lines) bending. (b) Change in size of the plates shown in (a) after further cooling. (c) Martensite plates (1) before and (2) after bending showing growth of one set of twins at the expense of the other. (d) Further growth of the martensite shown in C-2 due to further cooling.

Fig. 10. Microstructure of a tensile specimen given 8% total elongation at room temperature (a) Bright-field image and (b) dark-field image.

Fig. 11. Microstructure of a tensile specimen given 3% total elongation at room temperature (bright-field images).

Fig. 12. Scanning electron micrographs of the fracture surface of a tensile specimen tested at room temperature.

Fig. 13. Example of a hot-stage electron microscopy experiment showing skrinkage of martensite plates during heating (bright-field images and their corresponding diffraction patterns). (a) Room temperature (b) 200°C. (c) 250°C.

Fig. 14. Optical micrographs showing the effect of complete transformation cycles. (a) Initial microstructure (b) same area of (a) after immersion in liquid nitrogen for 20 minutes, heating to 100°C, cooling back to room temperature and slightly re-etching. (c) same area after 10 such cycles.

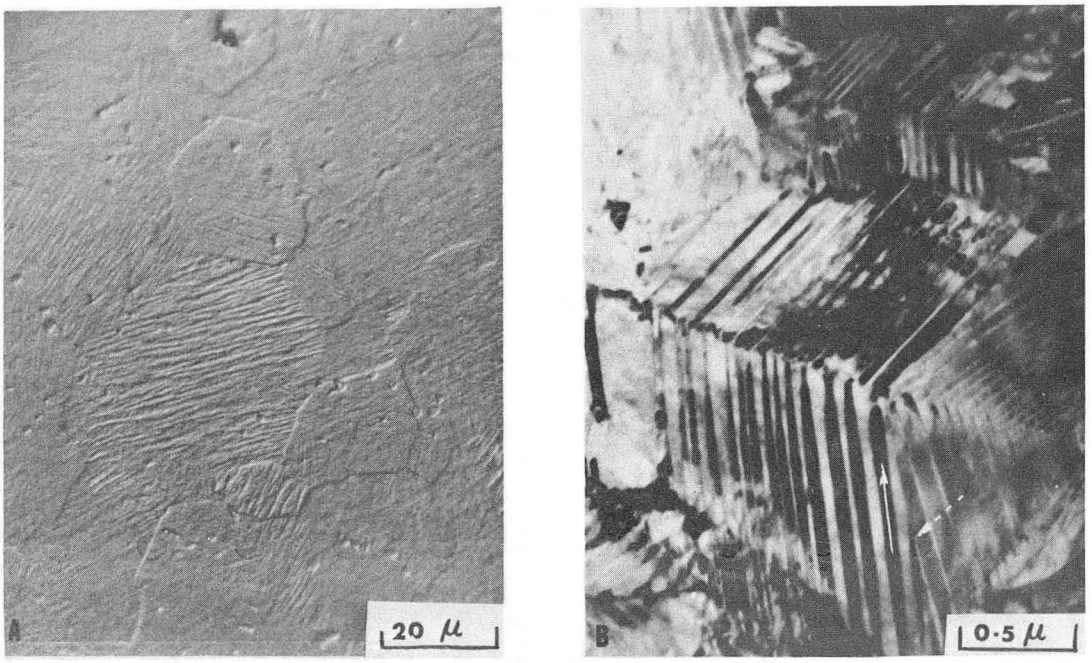

XBB 765-3848

FIG. 1

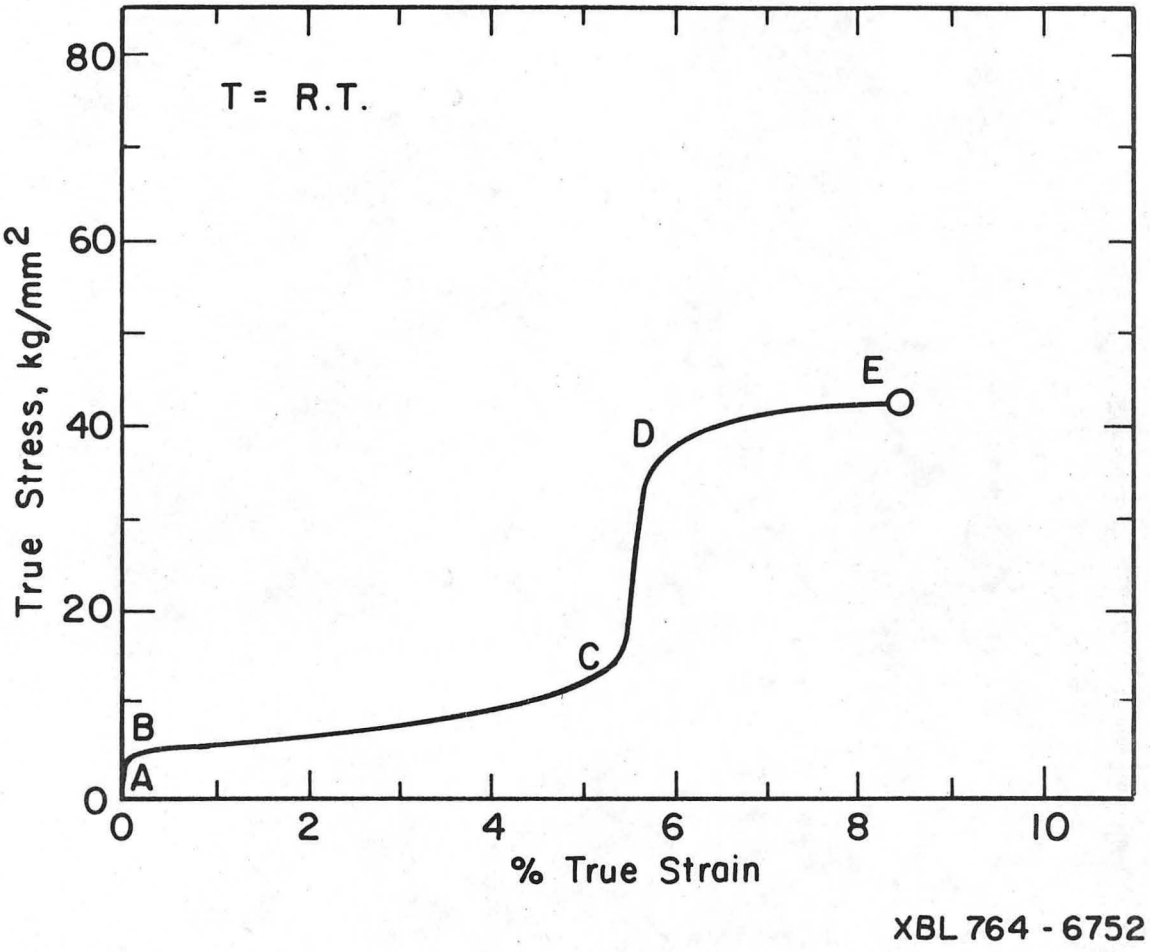

FIG. 2

XBB 765-3843

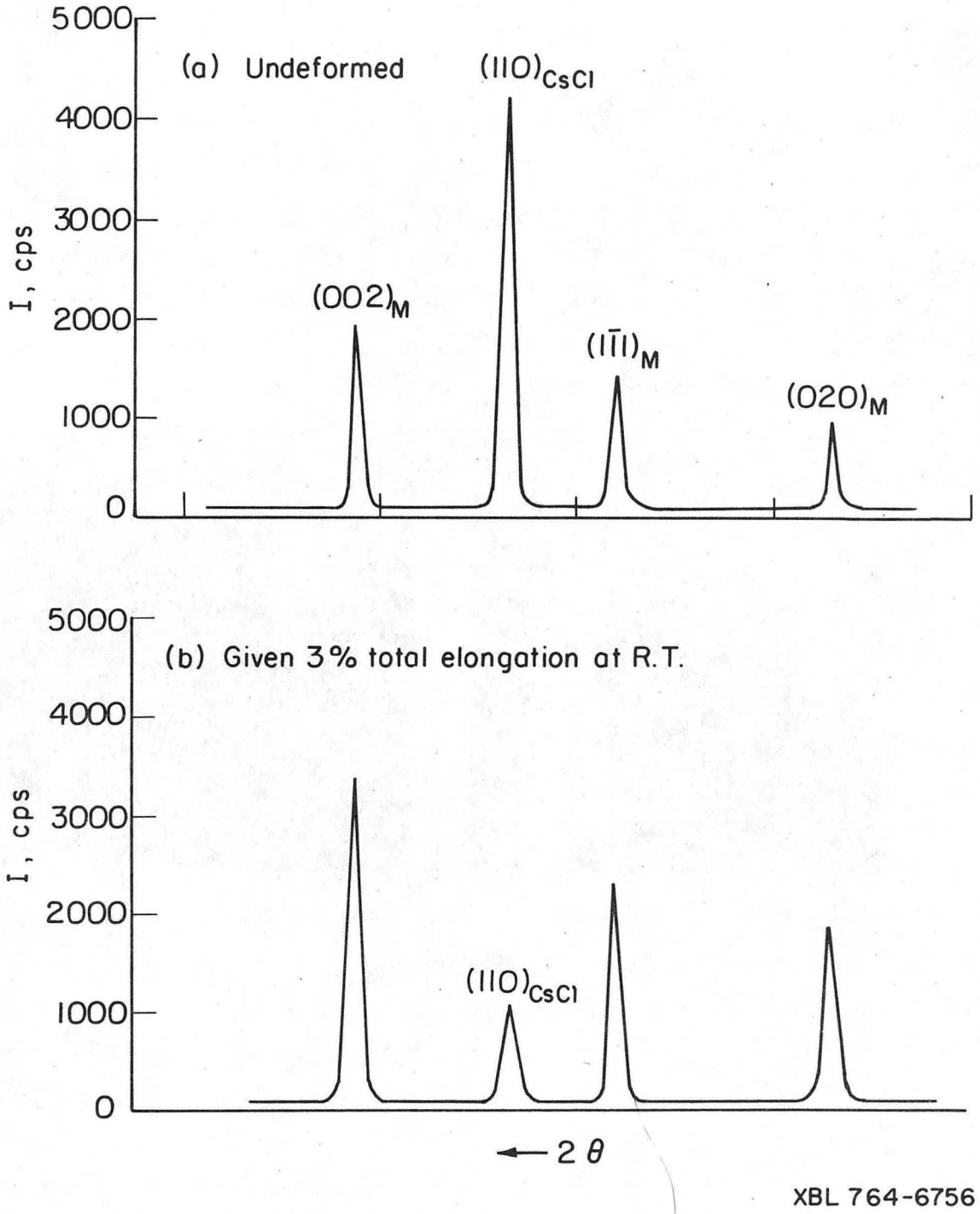

FIG. 4

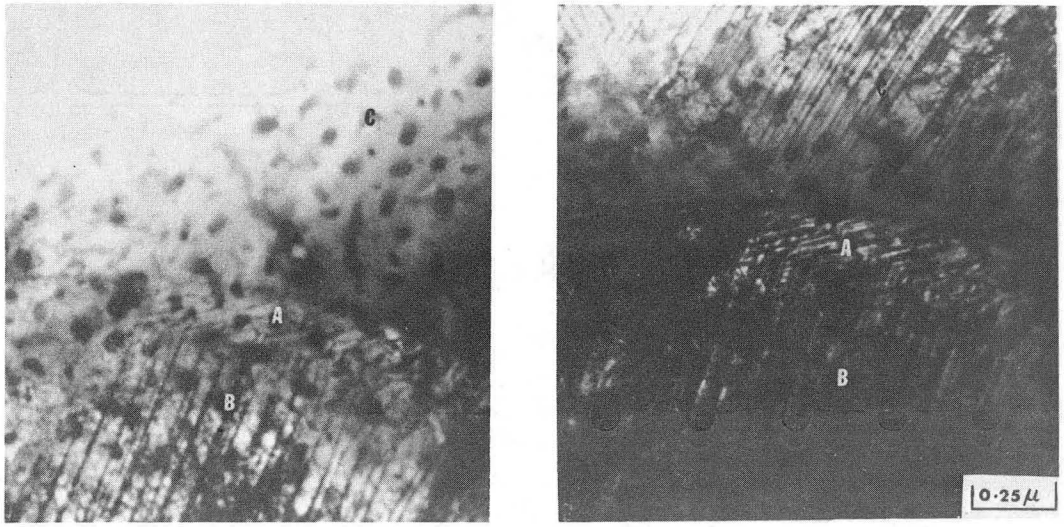

XBB 765-3847

FIG. 5

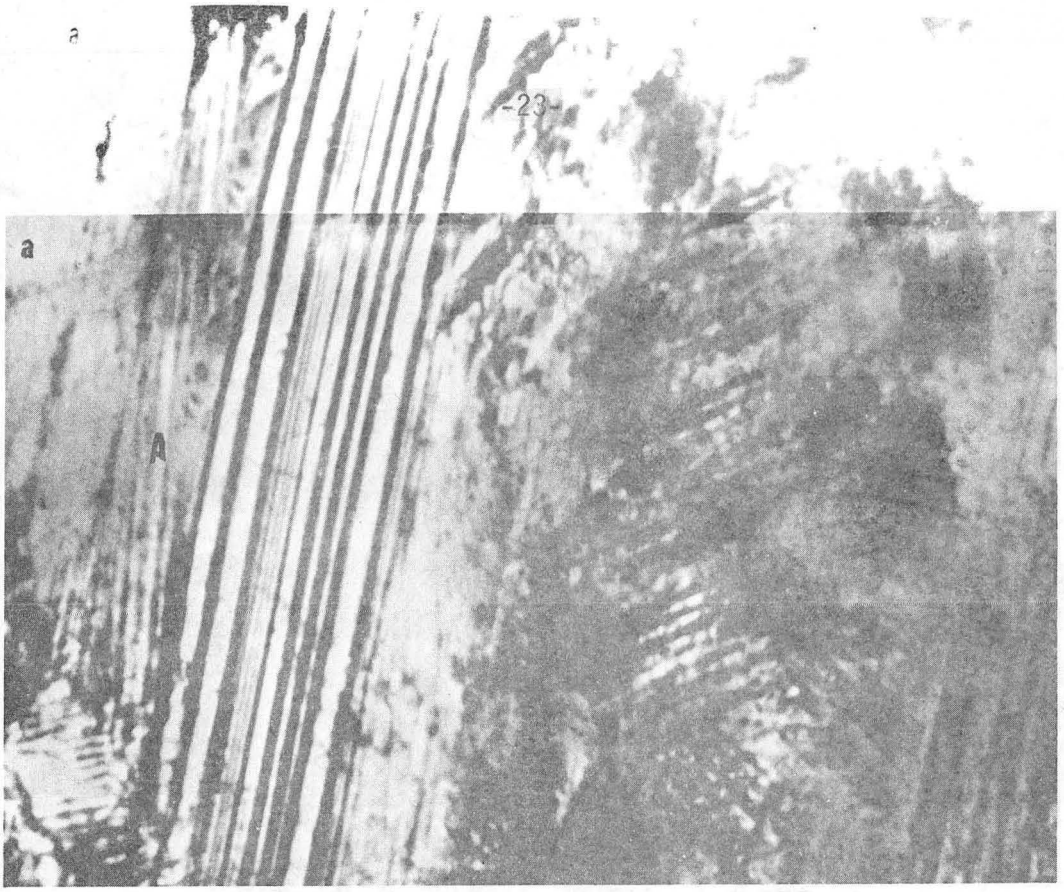

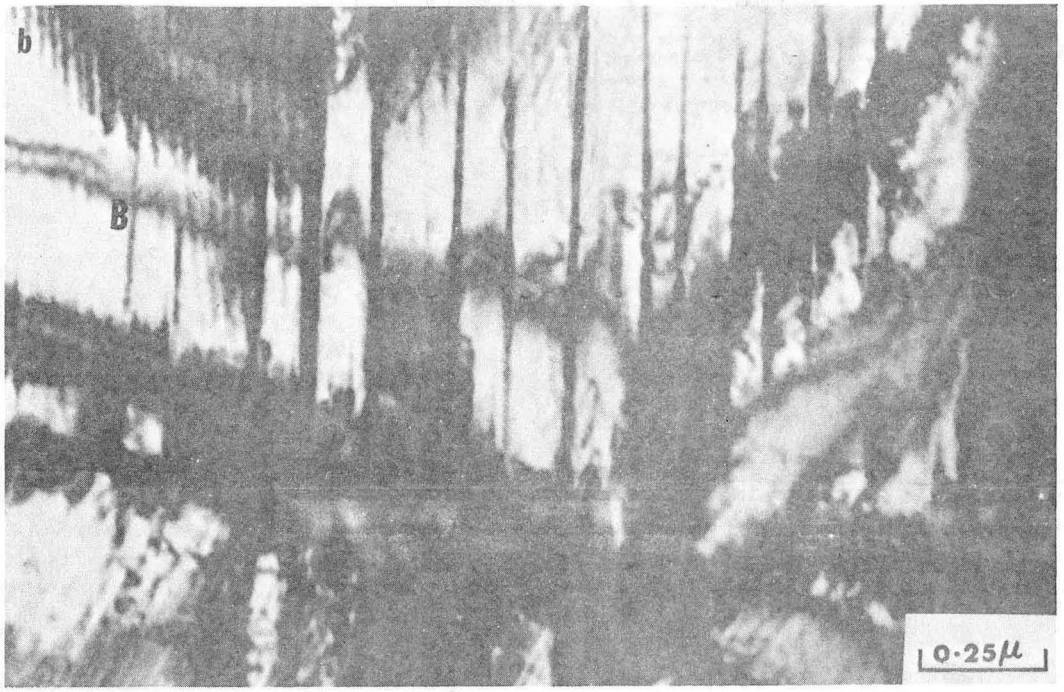

XBB 765-3849

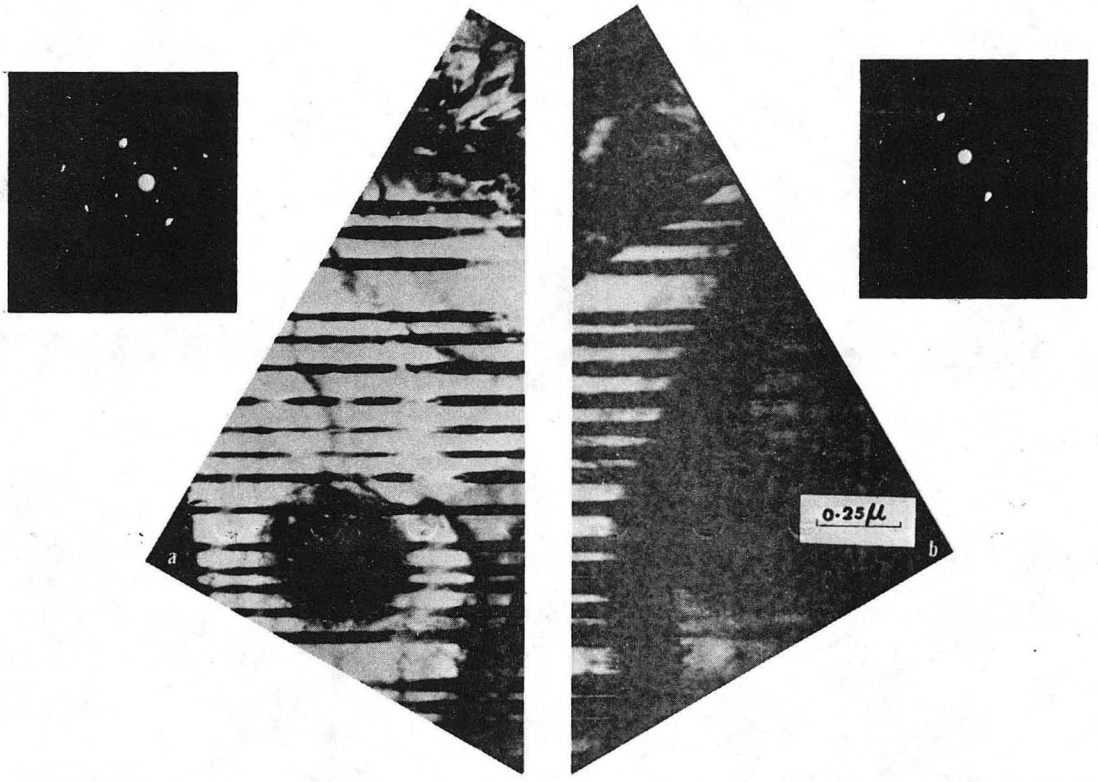

XBB 765-3846

FIG. 7

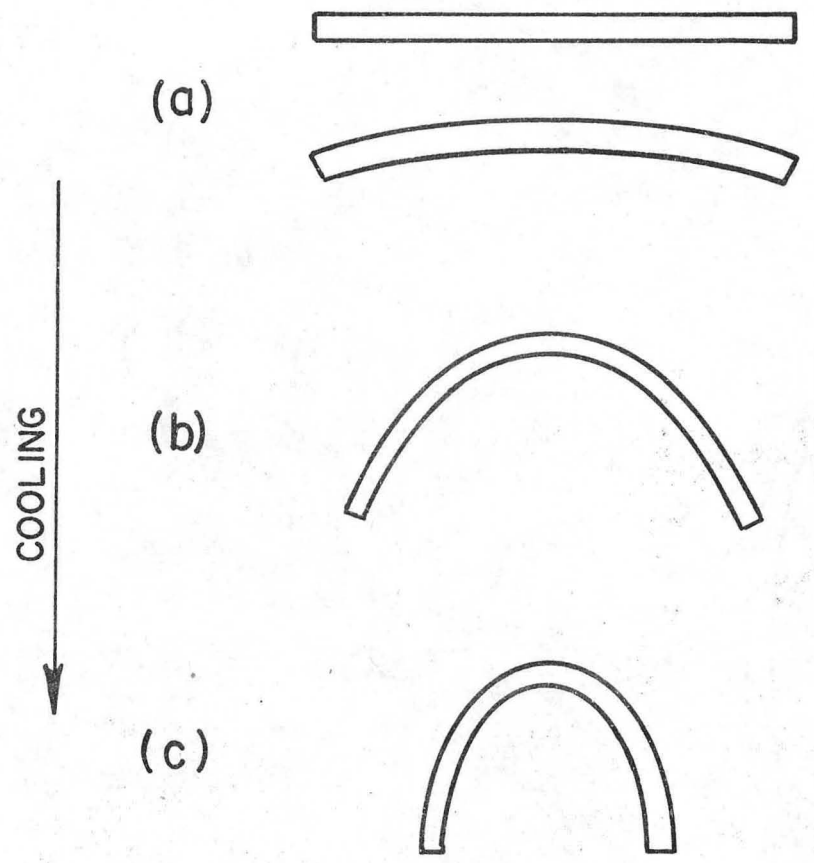

FIG. 8

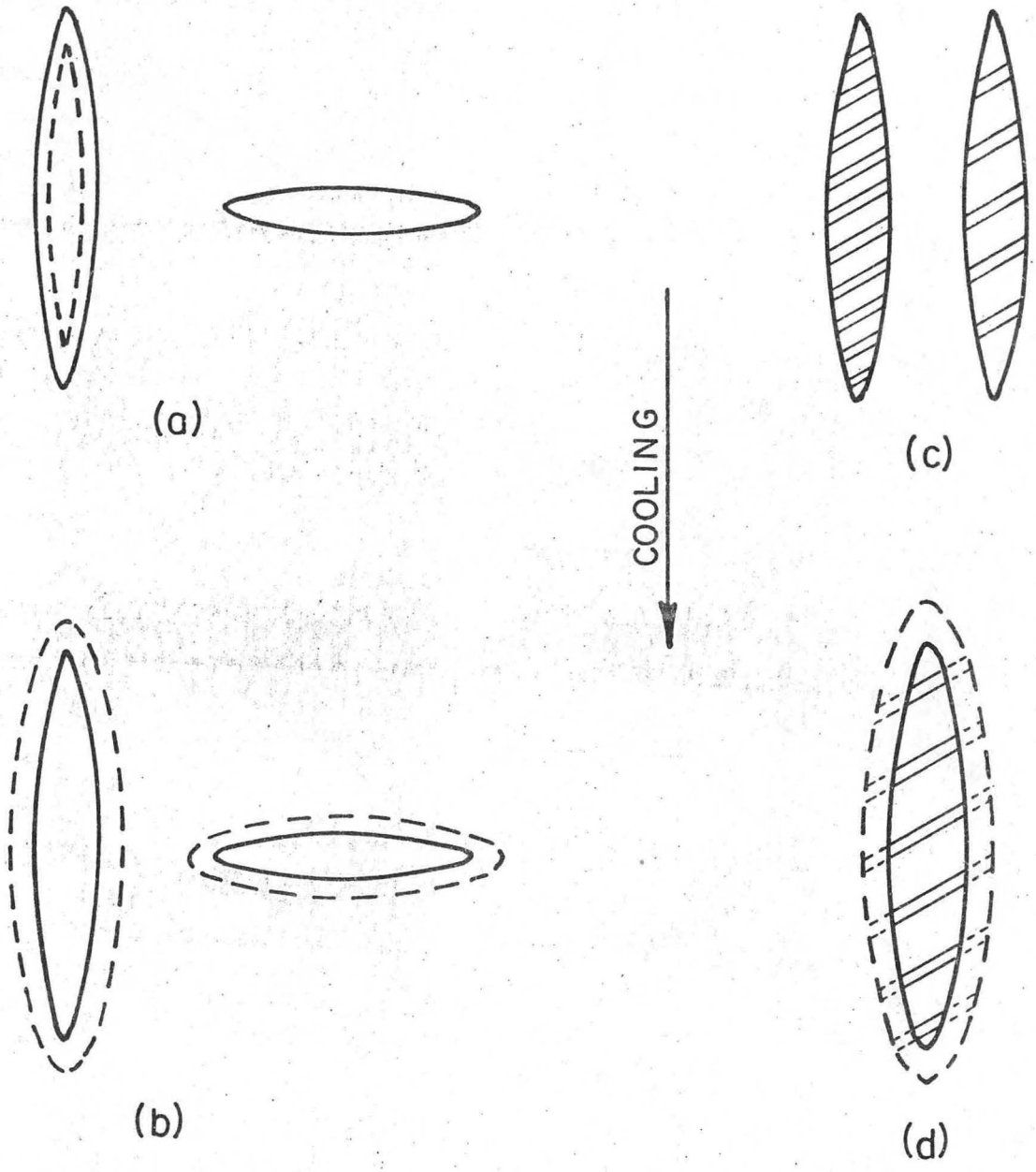

FIG. 9

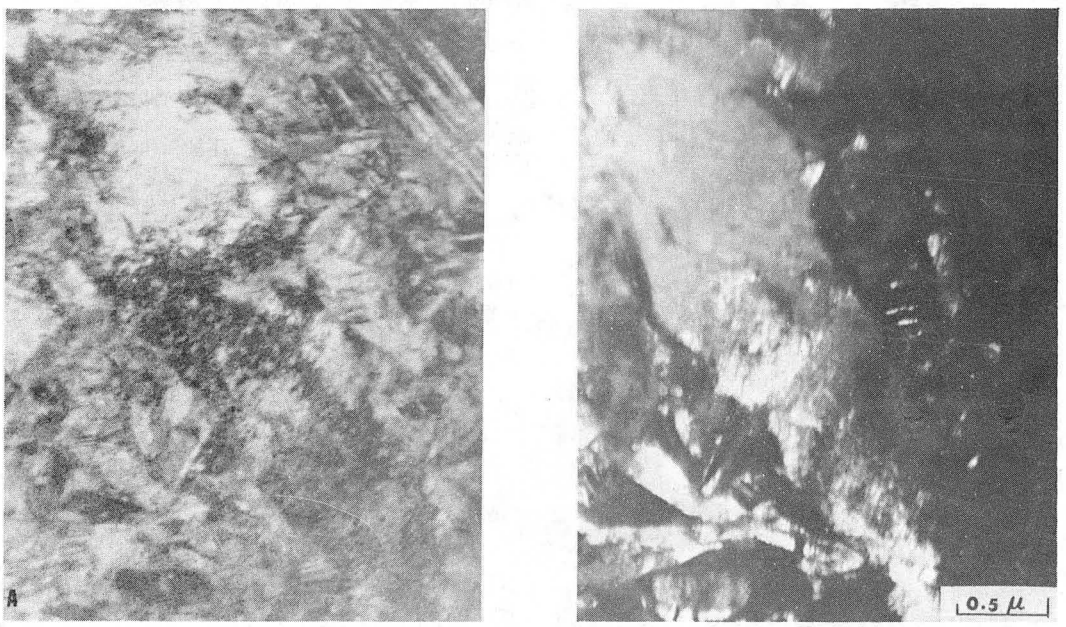

XBB 765-3862

FIG. 10

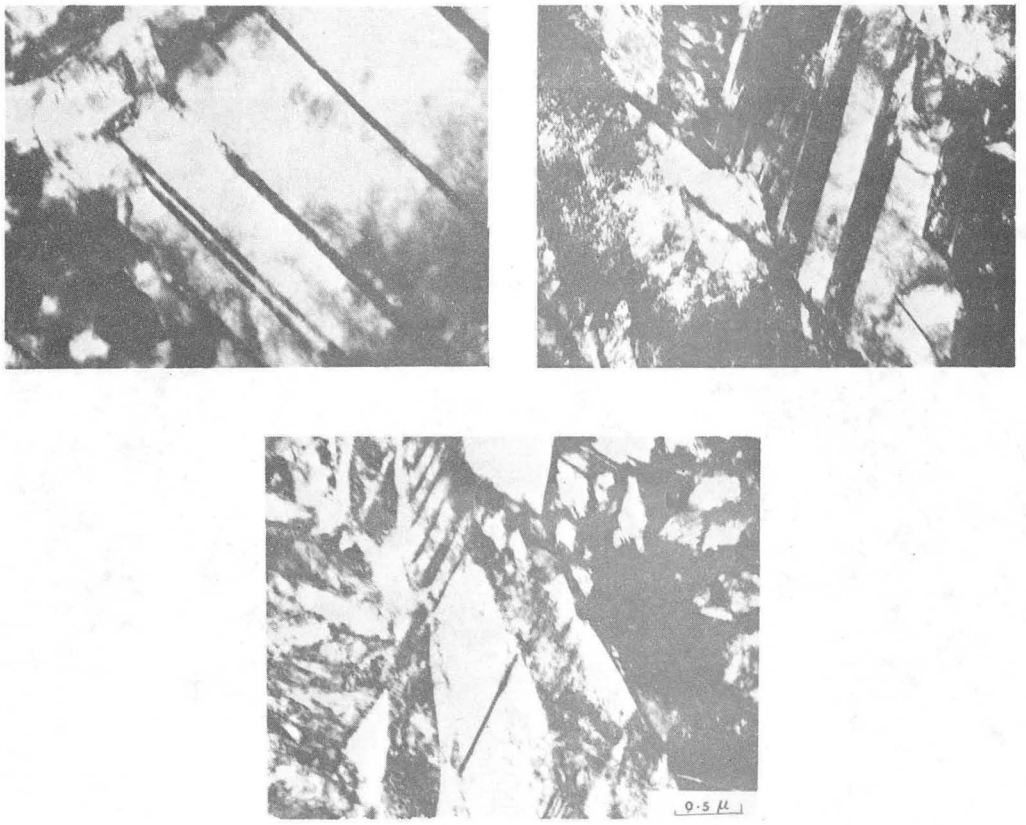

XBB 765-3856

Fig. 11

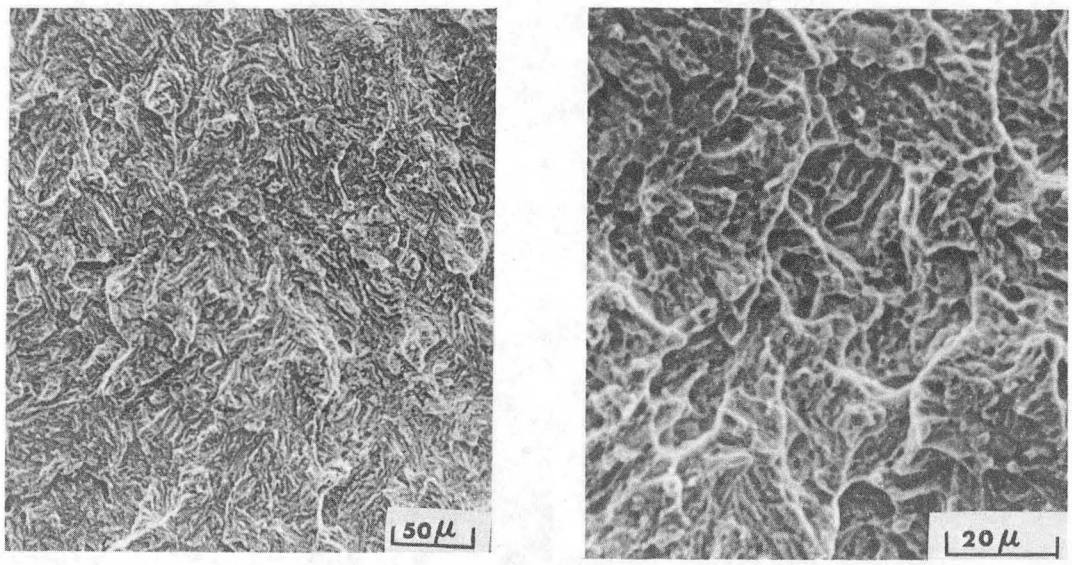

XBB-765-3851

FIG. 12

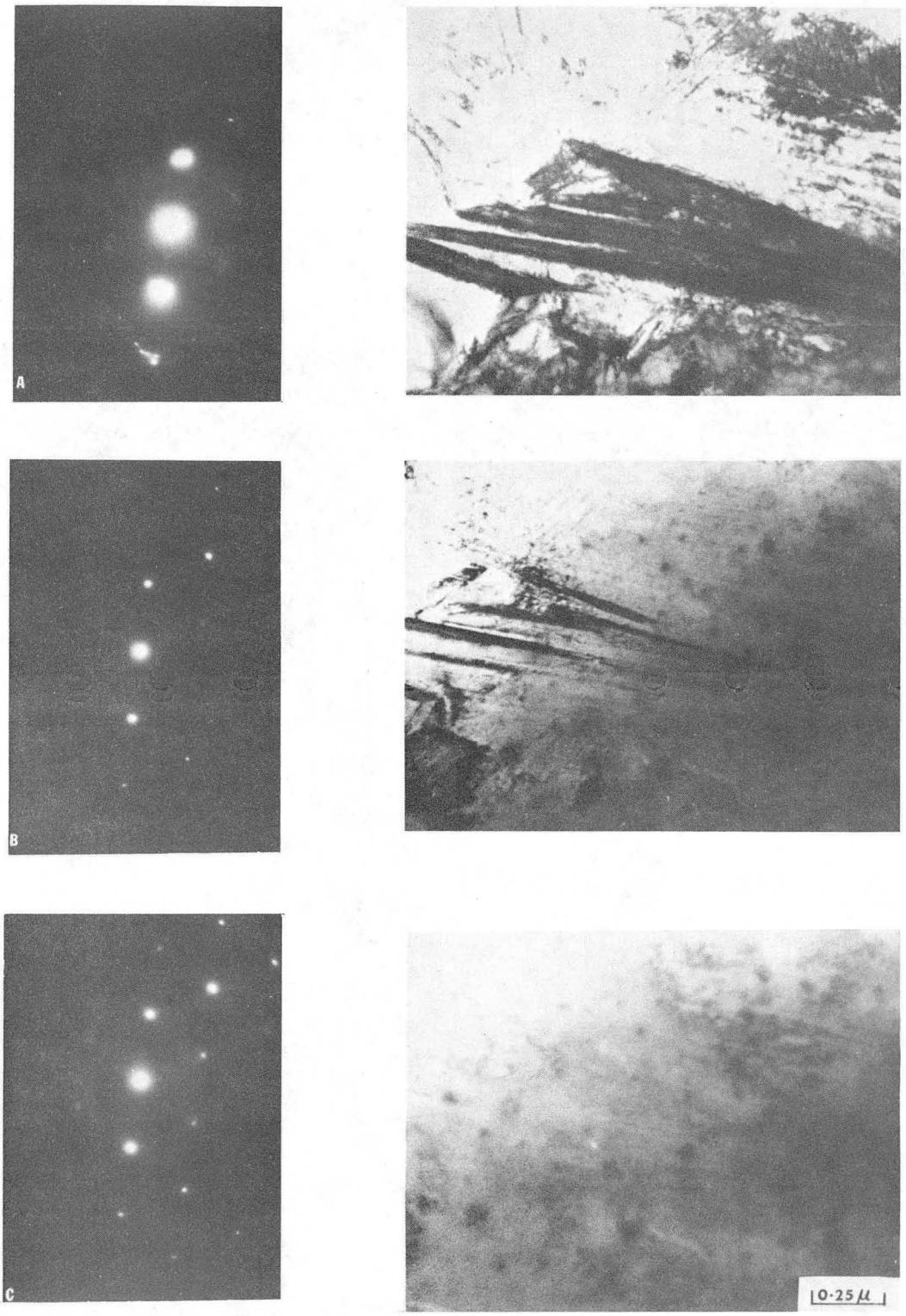

XBB 765-4045

FIG. 13

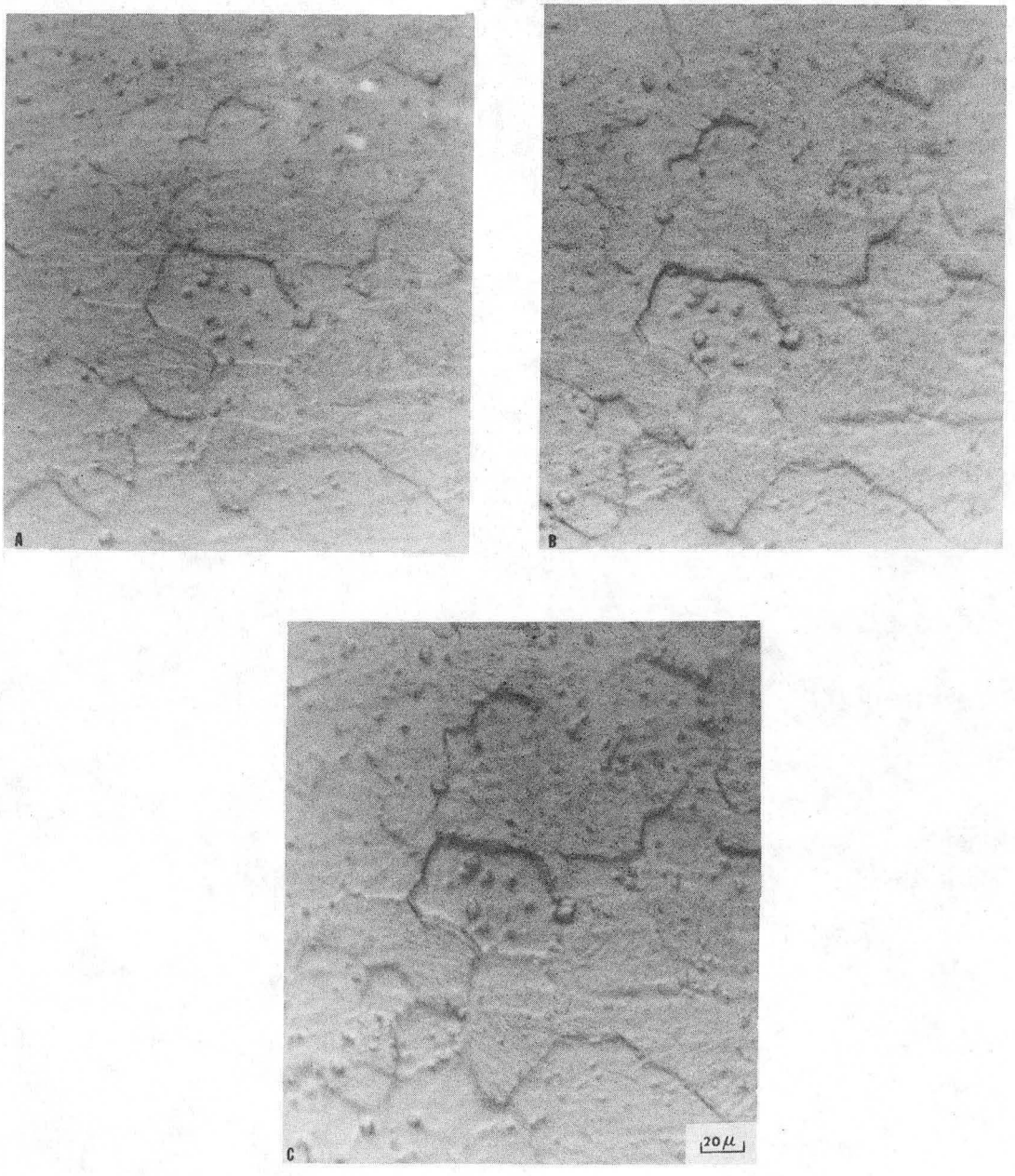

XBB-765-3844

TECHNICAL INFORMATION DIVISION
LAWRENCE BERKELEY LABORATORY
UNIVERSITY OF CALIFORNIA
BERKELEY, CALIFORNIA 94720